East European Journal of Physics. **1.** 116-122 (2022)
DOI:10.26565/2312-4334-2022-1-16 ISSN 2312-4334

RESOLUTION OF THE ULTRASOUND DOPPLER SYSTEM USING COHERENT PLANE-WAVE COMPOUNDING TECHNIQUE[†]

Iryna V. Sheina*, Eugen A. Barannik
Department of Medical Physics and Biomedical Nanotechnologies, V.N. Karazin Kharkiv National University
4, Svobody Sq., 61022, Kharkiv, Ukraine
**Corresponding Author: i.sheina@karazin.ua*
Received June 10, 2021; revised February 10, 2022; accepted March 14, 2022

In this work, in the process of plane-wave ultrasound probing from different angles the attainable spatial resolution was estimated on the basis of the previously developed theory of the Doppler response formation. In the theoretical calculations coherent compounding of the Doppler response signals was conducted over the period of changing the steering angles of probing. For this case an analytical expression for the ultrasound system sensitivity function over the field, which corresponds to the point spread function, is obtained. In the case of a rectangular weighting window for the response signals, the resolution is determined by the well-known sinc-function. The magnitude of the lateral resolution is inversely proportional to the range of the steering angles. It is shown that the theoretically estimated magnitude of the Doppler system lateral resolution, when using the technique of coherent plane-wave compounding, is in good agreement with the experimental data presented in literature.
Keywords: ultrasound imaging, Doppler spectra, synthetic aperture technique, coherent plane-wave compounding, continuum model of scattering, sensitivity function, point spread function, response formation.
PACS: 43.28.Py, 43.35.Yb, 43.60.-c, 87.63.D-, 87.63.dk

At present, along with the conventional techniques of ultrasound probing, some techniques, which use plane waves with different propagation directions [1-3] or wave fronts with a different spatial configuration, are rapidly developing [4, 5]. The essence of the technique is in the coherent compounding of the set of recorded ultrasound response signals for each point in space. The described principle of ultrasound probing is implemented, in particular, with the methods of synthetic aperture [4], coherent plane-wave compounding (CPWC) [3], as well as with their varieties and specific techniques [6-13].

The synthetic aperture data acquisition technologies allow achieving the best focusing at any point in the region of interest and obtain a sufficient amount of data for accurate resolution of flows velocity. The described advantages of the technique, in comparison with the conventional ultrasound one, are significant and make it possible to build full field-of-view tissue displacement and Doppler images at high frame rates and high resolution for various medical applications, including Dopplerography [8-11, 14-16], elastography [2, 3, 12, 13], and so on. However, application of these techniques requires massive computational demands, what entails an increase in the cost of medical equipment [17, 18]. Therefore, the task to develop new technique modifications, which can be easily integrated into the existing ultrasound systems and utilize the delay-and-sum hardware to reduce the computational costs and improve the image quality, remains highly relevant [6, 7]. It is also necessary to optimize the parameters that affect (characterize) the quality of images, obtained using the synthetic aperture technology [3, 11, 13, 15, 19-24].

The development of ultrasound Doppler techniques, with using the technology of coherent compounding of ultrasound response signals, made it possible to improve spectral estimations in comparison with those obtained, when using the conventional Doppler techniques [8]. A number of experimental works are devoted to the estimation of the velocity vector [9, 14, 22, 25], visualization of low-velocity blood flows [8, 10] and of small vessels [26], simultaneous visualization of blood flow and the vessel wall motion in the arteries [27], as well as the implementation of three-dimensional imaging for all the Doppler techniques (3-D ultrafast power Doppler, pulsed Doppler, color Doppler imaging) [11]. The effect of the influence of the ultrasound scatterers motion on the Doppler signal correlation function was theoretically investigated in [28], and in [23, 29] a motion correction scheme, which allowed to improve the accuracy of the velocity estimation, as well as to improve the signal-to-noise ratio, was developed. A number of experimental works are devoted to the development of new techniques within the frame of the plane-wave compounding technique, which allow improving the image quality in terms of lateral resolution, contrast ratio, and contrast-to-noise ratio both for two-dimensional B-mode (brightness mode) images [30-34] and for Doppler techniques [35-37].

Despite the existence of numerous theoretical and experimental works, devoted to the coherent compounding for Doppler applications, the studies of the best achievable spatial resolution of an ultrasound system are ongoing up to now, with using the Doppler method for determining the rate of motion. A general theory of the Doppler response formation was developed in [38, 39], which in [40] was generalized for the case of application of the technology of the emitted ultrasound beam dynamic focusing by the synthesized aperture method. In the present work, the spatial

[†] ***Cite as***: I.V. Sheina, and E.A. Barannik, East. Eur. J. Phys. **1**, 116 (2022), https://doi.org/10.26565/2312-4334-2022-1-16

resolution for the plane-wave coherent compounding was estimated on the basis of the previously developed theory of the Doppler response formation.

THEORETICAL MODEL

The present theoretical model of ultrasound scattering by biological tissues and fluids is based on the fact that these objects interact with the ultrasound field like an isotropic continuous medium [41, 42]. Within the framework of the continuum model, the ultrasound is scattered by the density inhomogeneities $\rho(\vec{r},t)$ and by the medium bulk compressibility $\beta(\vec{r},t)$, and the power spectrum of the Doppler response signal can be represented as in [39, 40, 43]

$$S(\omega)=k^4\int d\tau e^{i\omega\tau}\iint\limits_R e^{2i\vec{k}(\vec{r}_1-\vec{r}_0)}\overline{G_p'^{*}(\vec{r}_0,t_0)G_p'(\vec{r}_1,t_1)}C(\vec{r}_1-\vec{r}_0,\tau)d\vec{r}_0d\vec{r}_1, \tag{1}$$

$$C(\vec{r}_1-\vec{r}_0,\tau)=\left\langle\left(\tilde{\beta}(\vec{r}_0,t_0)-\tilde{\rho}(\vec{r}_0,t_0)\right)\left(\tilde{\beta}(\vec{r}_1,t_1)-\tilde{\rho}(\vec{r}_1,t_1)\right)\right\rangle,$$

where $\vec{k}$ and $k=2\pi/\lambda$ are the wave vector and wave number of the ultrasound transducer field in the plane-wave approximation, λ is the wavelength, $\langle\ldots\rangle$ is the mean value over the statistical ensemble, $\tau=t_1-t_0$, $\tilde{\rho}(\vec{r},t)=\rho^{-1}(\vec{r},t)\left[\rho(\vec{r},t)-\rho_0\right]$ and $\tilde{\beta}(\vec{r},t)=\beta_0^{-1}\left[\beta(\vec{r},t)-\beta_0\right]$ are the dimensionless fluctuations of the medium density and its volume compressibility relative to their space-time mean values ρ_0 and β_0, and the space-time characteristics of the density and compressibility fluctuations are described by the correlation function $C(\vec{r}_1-\vec{r}_0,\tau)$. The complex function of the distribution of the ultrasound system sensitivity $G_p'(\vec{r},t)$ over the field depends on the shape of the probing pulses, as well as on the amplitude and phase characteristics of the incident and reflected wave beams. When considering a synthesized aperture regardless of the method applied for determining the Doppler shift frequency and the spectra, described in [40, 43], in the known sensitivity function [41] its time dependence must be taken into account:

$$G_p'(\vec{r},t)=G_t'(\vec{r},t)G_r'(\vec{r},t)b\left(T_1-\frac{2x'(\vec{r})}{c(t)}\right), \tag{2}$$

where $b(t)$ is the envelope of the probing pulse, T_1 is the sampling time that determines the probing depth, $G_t'(\vec{r},t)$ and $G_r'(\vec{r},t)$ are the amplitude of incident waves and the function of the transducer sensitivity to the scattered waves, respectively, $x'(\vec{r})$ is the distance along the axis of transducer from its emitting surface to the origin of the coordinate system x,y,z in the region of interest, $c(t)$ is the propagation velocity of wave front along the axis $x'(\vec{r})$. The time dependence of the magnitude $c(t)$ arises due to the change in the direction of propagation of the emitted plane waves at different probings, as well as to different directions of the wave reception. As a result, in addition to averaging over the statistical ensemble, an averaging over the initial instant of time t_0 is necessary, which is indicated in expression (1) by the top line.

Two different feasible strategies for collection of information in the process of an ultrasound Doppler signal formation are described in [40], which utilize the dynamic change in the angles of radiation and the wave beam reception. For each case, general expressions were obtained for the Doppler signal power spectrum, whose width, according to the well-known Nyquist limit and the Rao-Cramer relation [41, 44], allows assessing the measurement accuracy of the Doppler spectrum average frequency. It was noted in [43], that the formation of the Doppler response directly from a sequence of response signals for the sequence of different directions could lead to broadening of the Doppler signal spectrum. In the physical sense, such a broadening has the same nature as that in the case of uniformly accelerated motion of ultrasound scatterers [45].

To the coherent compounding of discrete complex Doppler response signals at different directions of probing, their summation corresponds, in which the Doppler response is formed from such total values. In the first approximation, the summation can be replaced by integration over the period T of changing the directions of probing. In the case of coherent compounding, the Doppler spectrum width does not depend on the frequency-response characteristics of the sensitivity function [40]:

$$S(\omega_k)=\frac{k^4}{(2\pi)^3}T^2\int d\vec{q}C(\vec{q},\omega_k)\left|G(\vec{q}+2\vec{k},0)\right|^2, \tag{3}$$

where $G\left(\vec{q}+2\vec{k},\omega_i\right)$ is the Fourier-transform of the sensitivity function $G'_p\left(\vec{r},t\right), C\left(\vec{q},\omega_k\right)$ are the spectral components of the correlation function, ω_k are the Doppler shift frequencies of the scattered wave, and $\vec{q}$ is the scattering wave vector. This circumstance indicates the principal feasibility to combine the optimal parameters of the Doppler estimation of the blood *flow* velocity with a high spatial resolution.

RESULTS

Expression (3) establishes only a general relationship between the power spectrum of the ultrasound Doppler response signal with the scatterers' motion spectral characteristics and the sensitivity function of the system. In general case, the resolution of the ultrasound diagnostic system is determined by its point spread function (PSF). To demonstrate the advantages of the synthetic aperture technology over conventional methods in terms of improving the spatial resolution, let us analyze the function of sensitivity $\left|G'_p\left(\vec{r},\omega_i=0\right)\right|$. In the case, when the plane-wave coherent compounding is considereed, it is just this quantity that represents the PSF of the ultrasound diagnostic system. Therefore, the resolution at the given level can be estimated from the corresponding width of the sensitivity function $\left|G'_p\left(\vec{r},\omega_i=0\right)\right|$.

In the case of probing a biological medium by plane waves at different angles, the quantities $G'_t\left(\vec{r},t\right)$ and $G'_r\left(\vec{r},t\right)$ are time dependent due to the wave vector $\vec{k}\left(t\right)$, which changes with the change in the direction of probing in time (see Fig. 1, left). The propagation velocity of the plane-wave inclined front with the wave vector $\vec{k}\left(t\right)$ along the direction x' is equal to $c\left(t\right)=c_0/\cos\Phi\left(t\right)$, where c_0 is the equilibrium rate of ultrasound waves in the medium, $\Phi\left(t\right)$ is the angle between the direction of the wave vector $\vec{k}\left(t\right)$ and the axis x'. In accordance with this fact, the probing depth for the given sampling time is equal to $l_0=c_0T_1/2\cos\Phi$.

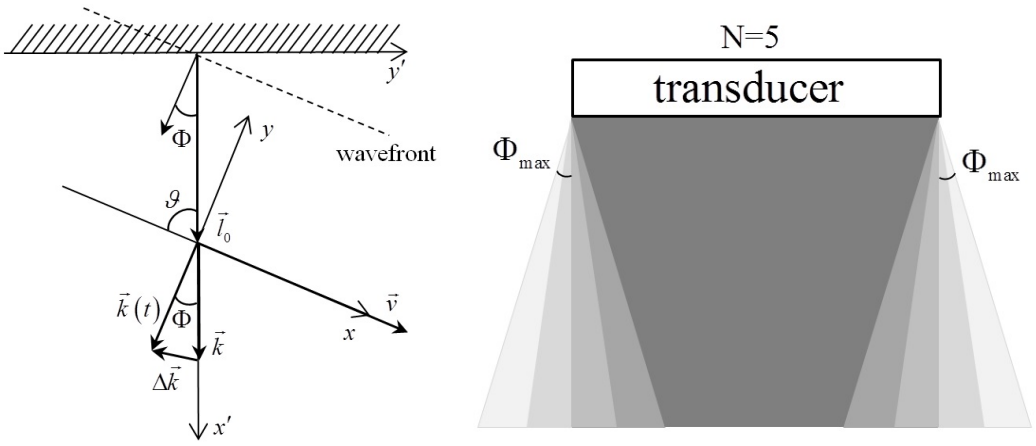

Figure 1. Relative position of the coordinate systems linked to the transducer and the region of interest, when probing with plane-wave fronts at different angles (left). Example of CPWC: five plane waves are transmitted and compounded. The least transparent region is the region with the highest resolution (right).

In the case of plane-wave fronts, the sensitivity function has the form:

$$G'_p\left(\vec{r},t\right)=G_0e^{2i\left\{\vec{k}(t)-\vec{k}\right\}\vec{r}}b\left(T_1-\frac{2x'\cos\Phi\left(t\right)}{c_0}\right), \tag{4}$$

where G_0 is a constant dimensional coefficient, $\vec{k}\left(t\right)$ is the direction wave vector, corresponding to time t, and its Fourier component can be described by the expression

$$G'_p\left(\vec{r},\omega_j\right)=\frac{G_0}{T}\int_{-T/2}^{T/2}e^{2i\left\{\vec{k}(t)-\vec{k}\right\}\vec{r}}b\left(T_1-\frac{2x'\cos\Phi\left(t\right)}{c_0}\right)e^{i\omega_jt}dt, \tag{5}$$

As a rule, in CPWC the angle $\Phi\left(t\right)$ at all steering angles can be considered small, then from Fig. 1 (left) it is obvious that the first term in the exponent of the integrand can be represented as

$$2\left\{\vec{k}\left(t\right)-\vec{k}\right\}\vec{r}\simeq2\Delta k\vec{e}_{y'}\vec{r}=2\Delta k\vec{e}_{y'}\left(\vec{r}'-\vec{l}_0\right)=2\Delta ky'=4k\sin\frac{\Phi\left(t\right)}{2}y'.$$

Then, substituting the last expression in (5), we obtain

$$G'_p\left(\vec{r},\omega_j\right)=\frac{G_0}{T}\int\limits_{-T/2}^{T/2}e^{4ik\sin\frac{\Phi(t)}{2}y'+i\omega_j t}b\left(T_1-\frac{2x'\cos\Phi(t)}{c_0}\right)dt\,. \tag{6}$$

Generally, in CPWC all the transmit angles are distributed symmetrically about 0° and equally spaces, as Fig. 1 (right) shows. As a result, the expression for the frequency component of the sensitivity function is reduced to the integral, which can be easily taken analytically. Then, when integrating (6), one can introduce the angular velocity of rotation of the wave vector $\vec{k}(t)$ in accordance with the law $\Phi(t)=\Omega t$. In addition, with the smallness of the angle Φ taken into account, one can use the expansion of the sine and cosine in the linear approximation in Φ.

$$G'_p\left(\vec{r},\omega_j\right)\cong\frac{G_0}{T}\int\limits_{-T/2}^{T/2}e^{4ik\frac{\Omega t}{2}y'+i\omega_j t}b\left(T_1-\frac{2x'}{c_0}\right)dt=G_0\frac{\sin\left(2k\Omega y'+\omega_j\right)\frac{T}{2}}{\left(2k\Omega y'+\omega_j\right)\frac{T}{2}}b\left(T_1-\frac{2x'}{c_0}\right). \tag{7}$$

In the general case of a dynamically changing radiation field, the Doppler signal is a sequence of discrete values of the response signals for the sequence of different angles, and the dependence on frequency_ω_j of the sensitivity function is described by expressions (5)-(7). This value has its maximum at the frequency component, which depends on the value of the transverse coordinate y': $\omega_j=-2k\Omega y'$. In the considered case of coherent plane-wave compounding, the sensitivity function takes the form:

$$G'_p\left(\vec{r},\omega_j=0\right)\cong G_0\frac{\sin k\Omega Ty'}{k\Omega Ty'}b\left(T_1-\frac{2x'}{c_0}\right). \tag{8}$$

We note right away, that in accordance with these expressions, the resolution in the transverse direction does not depend on the probing depth and is determined by the so-called sinc-function $\mathrm{sinc}(x)=\sin x/x$. Such a form is associated with the choice of the rectangular weighting function for the response signals at different steering angles. The use of other known weighting windows, when integrating in (6), allows suppressing the side lobes of the sensitivity function with some broadening of the main lobe.

Nevertheless, when using expression (8), it is easy to estimate the attainable resolution. In particular, the first zero of the sensitivity function appears at such a value of the transverse coordinate, which satisfies the equality $k\Omega Ty'_0=\pi$.

Here we obtain the width of the sensitivity function

$$d=2y'_0=2\frac{\lambda}{2\Omega T}=\frac{\lambda}{2\Phi_{\max}}, \tag{9}$$

where $2\Phi_{\max}$ is the entire range of the steering angles, i.e. the angle between the extreme directions of the wave vector.

In a number of experimental works [30, 35], the full width at half maximum (FWHM, -6 dB beam width), which characterizes the main lobe of the directivity diagram, is used to estimate the resolution for the point targets both in the longitudinal and transverse directions. The numerical estimate for the sensitivity function width at the level of 6 dB gives the value

$$d_{6dB}=2y'_{6dB}\approx\frac{0.3\lambda}{\Phi_{\max}}, \tag{10}$$

Where y'_{6dB} is the root of the equation $\sin y'_{6dB}=\frac{1}{2}y'_{6dB}$ along the interval $0\le y'_{6dB}\le\pi$.

DISSCUSSION

Generally, the CPWC uses a sequence of N of several consecutive emissions of broad wave beams at different angles Φ (see Fig. 1 (right)). As it follows from expressions (9)-(10), the Doppler system lateral resolution depends only on the maximum angle $\Phi_{\max}$, but not on the number N of the probing angles. For this reason, an increase in the frame rate at the same resolution can be obtained by decreasing the number of probing angles (without changing the value of the maximum probing angle).

However, the number of insonifications of the medium significantly affect the image contrast and the signal-to-noise ratio [3, 35]. It is the expression (3) that shows the response signal power to be proportional to the value T^2, which actually represents the square of the value N of the number of probing wavefronts over time T. Therefore, a

decrease in the value N, while maintaining the value of the maximum angle leads to a decrease in the contrast [35], and the signal-to-noise ratio increases with an increase of N, as long as, when summing the random noise, its power increases by N times, what results in the signal-to-noise ratio to be proportional to N, which corresponds to [3].

If assuming $\Delta\alpha = \pi/12$, then from (9) and (10) we obtain $d \simeq 2\lambda$ and $d_{6dB} \simeq 1.2\lambda$, respectively, which correspond to the values, which are usual for the lateral resolution in the focal region of the standard system. Thus, in [35] the central frequency was equal to $8MHz$, which corresponded to the wavelength $\lambda = 0.1925mm$, $\Delta\alpha = 12^\circ = \pi/15$, and the resolution was in the range from $0.33mm$ (at the probing depth of $1\,cm$) to $0.50mm$ (at the probing depth of $2.8\,cm$). The resolution values, calculated according to expressions (9) and (10), are equal to $d \approx 0.46mm$ and $d_{6dB} \approx 0.28mm$, respectively.

Strictly speaking, when using the synthetic aperture technique, the width of the measuring volume is determined not only by the functions $G_t'(\vec{r},t)$ and $G_r'(\vec{r},t)$, but also, to a small extent, by the probing pulse duration. This effect can be taken into account, if in the expression for the Fourier component of the sensitivity function (6), the expansion is carried out up to the quadratic ones by Φ terms in the argument of the pulse envelop, what will result in additional weak time dependence.

The estimates of the Doppler system lateral resolution show that, in contrast to the traditional Doppler methods, the attainable lateral resolution, when the technique of the coherent plane-wave compounding in the entire range of the probing depth is applied, is not worse than that in the focal region at the traditional ultasonic focusing. Such methods as ultrafast power Doppler imaging (Coherent Flow Power Doppler – CFPD) [10] make it possible to evaluate low-velocity blood flows in small vessels (<1mm). Color Doppler mapping in small vessels is extremely important, for example, in clinical cases of the development of abnormal growth of vessels structures, such as angiogenesis in cancer [46], or those caused by inflammation processes [47]. The varieties of Doppler techniques allow suppressing incoherent noises and artifacts, associated with the biological structures motion, thereby significantly improving the quality of the resulting image, what is confirmed by clinical investigations [48, 49].

From the point of view of spectral estimates, when using the technology of coherent plane-wave compounding, it is necessary to determine properly the total Doppler power spectrum. To obtain the corresponding analytical expression, the integral in expression (3) should be calculated using the expression for the sensitivity function (8), which was obtained in the present work. The solution to this problem is beyond the scope of this work and is of interest for further studies of the CPWC method.

CONCLUSIONS

Improving the quality of biological object images, obtained by ultrasound Doppler studies, is an urgent task. The problem of low- flow imaging in small vessels is especially acute, when using traditional imaging techniques, where the feasibility of clutter filtering is a major challenge, since only a small number of temporary samples are available for processing.

The appearance of the new technique for the coherent plane-wave compounding has provided a better quality of B-images and the possibility of continuous collection of information for the Doppler modes, as compared to the traditional techniques. The technique allows to build the full field-of-view tissue displacement and Doppler images at high frame rates and high resolution, while continuous data collection provides new opportunities for clutter filtering and imaging the low-velocity flows. In accordance with the CPWC technology, a high-resolution image is formed by coherent compounding of ultrasound response signals, obtained from a set of probing pulses from different steering angles.

In this work, an estimation of the achievable spatial resolution was carried out with using the CPWC technology based on the previously developed theory of the Doppler response formation with a dynamic change in the direction of ultrasound waves. An analytical expression has been obtained for the ultrasound system field sensitivity, which in the case of a rectangular weighting window for the response signals is determined by the sinc-function, well known from the theory of focusing. The magnitude of the lateral resolution, which is inversely proportional to the range of the steering angles, does not depend on the total number of the steering angles and the probing depth. It is shown that the theoretically estimated magnitude of the Doppler system lateral resolution, when using the coherent plane-wave compounding, is no worse than that in the focal region with the traditional focusing of ultrasound, and is in good agreement with the experimental data presented in literature.

ORCID IDs

Iryna V. Sheina, https://orcid.org/0000-0002-0293-4849; **Evgen A. Barannik,** https://orcid.org/0000-0002-3962-9960

REFERENCES

[1] J.Y. Lu, IEEE Trans. Ultrason., Ferroelec., Freq. Contr. **44**(4), 839 (1997), https://doi.org/10.1109/58.655200

[2] M. Tanter, J. Bercoff, L. Sandrin, and M. Fink, IEEE Trans. Ultrason. Ferroelectr.Freq. Contr.**49**(10), 1363 (2002), https://doi.org/10.1109/TUFFC.2002.1041078

[3] G. Montaldo, M. Tanter, J. Bercoff, N. Benech, and M. Fink, IEEE Trans. Ultrason.Ferroelectr.Freq.Contr. **56**(3), 489 (2009), https://doi.org/10.1109/TUFFC.2009.1067

[4] J.A. Jensen, S.I. Nikolov, K.L. Gammelmarkand, and M.H. Pedersen, Ultrasonics, **44**(1), e5 (2006), https://doi.org/10.1016/j.ultras.2006.07.017
[5] J.-l. Gennisson et al., IEEE Trans. Ultrason. Ferroelec. Freq. Contr. 62(6), 1059 (2015), https://doi.org/10.1109/TUFFC.2014.006936
[6] M. A. Lediju, G. E. Trahey, B. C. Byram and J. J. Dahl, IEEE Trans. Ultrason. Ferroelec. Freq. Contr. **58**(7), 1377 (2011), http://doi.org/10.1109/TUFFC.2011.1957
[7] Y.L. Li, J.J. Dahl, J. Acoust. Soc. Am. **141**(3), 1582 (2017), https://doi.org/10.1121/1.4976960
[8] J. Bercoff, G. Montaldo, T. Loupas, D. Savery, F. Meziere, M. Fink, and M. Tanter, IEEE Trans. Ultrason. Ferroelec. Freq. Contr. **58**(1), 134 (2011), https://doi.org/10.1109/TUFFC.2011.1780
[9] J. A. Jensen and N. Oddershede, IEEE Trans. Med. Imag. **25**(12), 1637-1644(2006), https://doi.org/10.1109/TMI.2006.883087
[10] Y.L. Li, J.J. Dahl, IEEE Trans. Ultrason. Ferroelec. Freq. Contr. **62**(6), 1022 (2015), https://doi.org/10.1109/TUFFC.2014.006793
[11] [11] J. Provost, C. Papadacci, C. Demene, J. Gennisson, M. Tanter and M. Pernot, IEEE Trans. Ultrason. Ferroelec. Freq. Contr. **62**(8), 1467 (2015), https://doi.org/10.1109/TUFFC.2015.007032
[12] J. Bercoff , M. Tanter, and M. Fink, IEEE Trans. Ultrason. Ferroelec. Freq. Contr. **51**(4), 396 (2004), https://doi.org/10.1109/TUFFC.2004.1295425
[13] C. Papadacci, M. Pernot, M. Couade, M. Fink and M. Tanter, IEEE Trans. Ultrason. Ferroelec. Freq. Contr. 61(2), 288 (2014), http://doi.org/10.1109/TUFFC.2014.6722614
[14] J. Udesen, F. Gran, K. L. Hansen, J. A. Jensen, C. Thomsen and M. B. Nielsen, IEEE Trans. Ultrason. Ferroelec. Freq. Contr., **55**(8), 1729 (2008), https://doi.org/10.1109/TUFFC.2008.858
[15] J. Jensen, M. B. Stuart, and J. A. Jensen, IEEE Trans. Ultrason. Ferroelec. Freq. Contr. **63**(11), 1922 (2016), https://doi.org/10.1109/TUFFC.2016.2591980
[16] B. Osmanski, M. Pernot, G. Montaldo, A. Bel, E. Messas and M. Tanter, IEEE Trans. Med. Imag., **31**(8), 1661 (2012), http://doi.org/10.1109/TMI.2012.2203316
[17] M. Tanter and M. Fink, IEEE Trans. Ultrason. Ferroelectr. Freq. Control. **61**(1), 102 (2014), https://doi.org/10.1109/TUFFC.2014.6689779
[18] S. I. Nikolov, B. G. Tomov and J. A. Jensen, *2006 Fortieth Asilomar Conference on Signals, Systems and Computers*, 2006, pp. 1548-1552, https://doi.org/10.1109/ACSSC.2006.355018
[19] R. Moshavegh, J. Jensen, C. A. Villagómez-Hoyos, M. B. Stuart, M. C. Hemmsen and J. A. Jensen, in *Proceedings of SPIE Medical Imaging* (San Diego, California, United States, 2016) pp. 97900Z-97900Z-9, https://doi.org/10.1117/12.2216506
[20] J. Kortbek, J. A. Jensen and K. L. Gammelmark, Ultrasonics, **53**(1), 1 (2013), https://doi.org/10.1016/j.ultras.2012.06.006
[21] J. Cheng and J.Y. Lu, IEEE Trans. Ultrason. Ferroelec. Freq. Contr. **53**(5), 880 (2006), https://doi.org/10.1109/TUFFC.2006.1632680
[22] N. Oddershedeand J. A. Jensen, IEEE Trans. Ultrason. Ferroelec. Freq. Contr. **54**(9), 1811 (2007), https://doi.org/10.1109/TUFFC.2007.465
[23] B. Denarie et al., IEEE Trans. Med. Imaging **32**(7), 1265 (2013), https://doi.org/10.1109/TMI.2013.2255310
[24] Y. Tasinkevych, I. Trots, A. Nowicki, P.A. Lewin, Ultrasonics **52**(2), 333 (2012), https://doi.org/10.1016/j.ultras.2011.09.003
[25] S. Ricci, L. Bassi and P. Tortoli, IEEE Trans. Ultrason. Ferroelec. Freq. Contr. **61**(2), 314 (2014), https://doi.org/10.1109/TUFFC.2014.6722616
[26] Y. L, Li, D. Hyun, L. Abou-Elkacem, J. K. Willmann, J.J. Dahl, IEEE Trans. Ultrason. Ferroelec. Freq. Contr. **63**(11), 1878 (2016), https://doi.org/10.1109/TUFFC.2016.2616112
[27] I. K. Ekroll, A. Swillens, P. Segers, T. Dahl, H. Torp and L. Lovstakken, IEEE Trans. Ultrason. Ferroelec. Freq. Contr. **60**(4), 727 (2013) https://doi.org/10.1109/TUFFC.2013.2621
[28] D. Hyun, J.J. Dahl, J. Acoust. Soc. Am. **147**(3), 1323 (2020), https://doi.org/10.1121/10.0000809
[29] I.K. Ekroll, M.M. Voormolen, O.K.-V. Standal, J.M. Rau and L. Lovstakken, IEEE Trans. Ultrason. Ferroelec. Freq. Contr. **62**(9), 1634 (2015), https://doi.org/10.1109/TUFFC.2015.007010
[30] Y. Wang, C. Zheng, H. Peng and C. Zhang, IEEE Access **6**, 36927 (2018), https://doi.org/10.1109/ACCESS.2018.2852641
[31] S. Salles, F. Varray, Y. Bénane and O. Basset, *2016 IEEE International Ultrasonics Symposium (IUS)*, 2016, pp. 1-4, https://doi.org/10.1109/ULTSYM.2016.7728751
[32] C. Zheng, Q. Zha, L. Zhang and H. Peng, IEEE Access **6**, 495 (2018), https://doi.org/10.1109/ACCESS.2017.2768387
[33] Y.M. Benane et al., *2017 IEEE International Ultrasonics Symposium (IUS)*, 2017, pp. 1-4, https://doi.org/10.1109/ULTSYM.2017.8091880
[34] X. Yan, Y. Qi, Y. Wang, Y. Wang, Sensors **21**, 394 (2021), https://doi.org/10.3390/s21020394
[35] C. Golfetto, I. K. Ekroll, H. Torp, L. Løvstakken and J. Avdal, IEEE Trans. Ultrason. Ferroelec. Freq. Contr. **68**(4), 1105 (2021), https://doi.org/10.1109/TUFFC.2020.3033719
[36] S. Salles, H. Liebgott, O. Basset, C. Cachard, D. Vray and R. Lavarello, IEEE Trans. Ultrason. Ferroelec. Freq. Contr. **61**(11), 1824 (2014), https://doi.org/10.1109/TUFFC.2014.006543
[37] C.-C. Shen, Y.-C. Chu, Sensors **21**, 4856 (2021), https://doi.org/10.3390/s21144856
[38] E.A. Barannik, Ultrasonics **39**(2), 311 (2001), https://doi.org/10.1016/S0041-624X(01)00059-2
[39] I.V. Skresanova and E.A. Barannik, Ultrasonics **52**(5), 676 (2012), https://doi.org/10.1016/j.ultras.2012.01.014
[40] I.V. Sheina, O.B. Kiselov and E.A. Barannik, East Eur. J. Phys. **4**, 5 (2020), https://doi.org/10.26565/2312-4334-2020-4-01
[41] [41] P. J. Fish, in: *Physical Principles of Medical Ultrasonics*, editedby C.R. Hill (EllisHorwood, Chichester, 1986), pp. 338-376.
[42] R.J. Dickinson, D.K. Nassiri, in: *Physical principles of medical ultrasonics*, edited by C. R. Hill, J. C. Bamber, G. R. terHaar (John Wiley & Sons, West Sussex, 2004), pp. 191–222.
[43] E.A. Barannik and O.S. Matchenko, East Eur. J. Phys. **3**(2) 61 (2016), https://doi.org/10.26565/2312-4334-2016-2-08. (in Russian)

[44] W. Gilson andS. Orphanoudakis, in: *Proceedings of the Annual International Conference of the IEEE Engineering in Medicine and Biology Society* (IEEE, NewOrleans, 1988), pp. 473-474, https://doi.org/10.1109/IEMBS.1988.94615
[45] O.S. Matchenko and E.A. Barannik, Acoust. Phys. **63**(5), 596 (2017), https://doi.org/10.1134/S106377101705008
[46] R.S. Apte, D.S. Chen, N. Ferrara, Cell, **176(**6), 1248-1264 (2019), https://doi.org/10.1016/j.cell.2019.01.021
[47] J. Gallo, M. Raska, E. Kriegova, S. B. Goodman, Journal of Orthop. Translat., **10**, 52 (2017), https://doi.org/10.1016/j.jot.2017.05.007
[48] M. Jakovljevic, B.C. Yoon, L. Abou-Elkacem, D. Hyun, Y. Li, E. Rubesova, J.J. Dahl, IEEE Trans. Ultrason. Ferroelectr. Freq. Control. **68**(1), 92 (2021), https://doi.org/10.1109/TUFFC.2020.3010341
[49] Y.L. Li, D. Hyun, I. Durot, J.K. Willmann and J.J. Dahl, *2018 IEEE International Ultrasonics Symposium (IUS)*, 2018, pp. 1-9, https://doi.org/10.1109/ULTSYM.2018.8579726

РОЗДІЛЬНА ЗДАТНІСТЬ УЛЬТРАЗВУКОВОЇ ДОППЛЕРІВСЬКОЇ СИСТЕМИ ПРИ ВИКОРИСТАННІ ТЕХНОЛОГІЇ КОГЕРЕНТНОГО КОМПАУНДІНГУ ПЛОСКИХ ХВИЛЬ

І.В. Шеіна, Є.О. Баранник

Кафедра медичної фізики та біомедичних нанотехнологій, Харківський національний університет імені В.Н. Каразіна М. Свободи 4, Харків, 61022, Україна

В роботі на підставі розвиненої раніше теорії формування допплерівського відгуку проведені оцінки досяжної просторової роздільної здатності при ультразвуковому зондуванні плоскими хвилями з різних ракурсів. В теоретичних розрахунках когерентний компаундінг сигналів допплерівського відгуку проводився за періодом зміни ракурсів зондування. У цьому випадку здобуто аналітичний вираз для функції чутливості ультразвукової системи за полем, яка відповідає функції відгуку точкового джерела. У випадку прямокутного зважувального вікна для сигналів відгуку роздільна здатність визначається добре відомою sinc-функцією. Величина поперечної роздільної здатності обернено пропорційна діапазону ракурсних кутів. Показано, що теоретично оцінена величина поперечної роздільної здатності допплерівської системи при використанні технології когерентного компаундінгу плоских хвиль добре відповідає представленим в літературі експериментальним даним.

Ключові слова: ультразвукова візуалізація, допплерівський спектр, технологія синтезованої апертури, когерентний компаундінг плоских хвиль, континуальна модель розсіяння, функція чутливості, функція відгуку точкового джерела, формування відгуку